Side-Chain Copolymers Containing Smectic Monomer and Chiral Reagent—Synthesis and Characterization

Xiao-Zhi He, Bao-Yan Zhang, Jian-She Hu, Dan-Shu Yao, Zeng-Fu Hu

Center for Molecular Science and Engineering, Chemical Deparment, Northeastern University, Shenyang 110004, People's Republic of China

Received 26 April 2007; accepted 13 November 2007
DOI 10.1002/app.27670
Published online 23 January 2008 in Wiley InterScience (www.interscience.wiley.com).

ABSTRACT: A series of new chiral side-chain liquid-crystalline polymers were prepared containing smectic-nematic monomer and nonmesogenic chiral monomer. All polymers were synthesized by graft polymerization using polymethylhydrosiloxane as backbone. The mesomorphic properties were investigated by differential scanning calorimetry, polarizing optical microscopy, thermogravimetric analyses, and X-ray diffraction measurements. The chemical structures of the monomers and polymers obtained were confirmed by Fourier transform infrared, proton nuclear magnetic resonance spectra (^{1}H NMR). $\mathbf{M_1}$ showed smectic (S_B, S_C) and nematic phase on the heating and the cooling cycle. Polymers $\mathbf{P_0}$–$\mathbf{P_2}$ were in chiral smectic A phase, while $\mathbf{P_3}$–$\mathbf{P_5}$ were in cholesteric phase, $\mathbf{P_6}$ has bad LC properties, and $\mathbf{P_7}$ has no LC properties. Experimental results demonstrated that nonmesogenic chiral moiety and LC mesogenic with long carbochain offered the possibility of application because of its lower glass transition temperature, and the glass transition temperatures and isotropization temperatures and the ranges of the mesophase temperature reduced with increasing the contents of chiral agent. © 2008 Wiley Periodicals, Inc. J Appl Polym Sci 108: 1265–1272, 2008

Key words: chiral agent; glass transition; synthesis; liquid-crystalline polymers

INTRODUCTION

As it is known that the aim of our study generally is to understand the relationships between the molecular structure and the resulting macroscopic material properties.[1–3] To obtain this goal, copolymers are often combined by different molecular fragments and give rise to different properties in one material.[4–6]

Chiral liquid-crystalline phases (cholesteric or chiral smectic C phase) have attracted much interest. They have been extensively studied during the last century because of the unique properties and the potential ferroelectric properties, respectively.[7–15] And now it is also in the ascendant. Generally speaking, cholesteric phase was prepared by the copolymerization of a nematogenic monomer and a chiral monomer containing a rigid core to form the so-called induced cholesteric liquid-crystalline phase, and chiral smectic was obtained by the copolymerization of a smectic monomer and a chiral monomer.[6,16–20]

In our previous work, it has been reported that the synthesis and the properties of side-chain chiral LC were derived from cholesteric or nematic monomer with chiral agent.[21–23] The most common chiral agent so far considered for the synthesis of chiral side-chain LC polymers are cholesterol, menthol, acid with chiral group, and so on, while isosorbide has been much used for the synthesis of chiral main-chain LC polymers and little used for the synthesis of chiral side-chain LC polymers.[13] Therefore, it has been necessary to synthesize various kinds of side-chain chiral LC containing isosorbide to study the relationship between structure and properties and then explore their potential application. And at the same time, the synthesis of lower T_g cholesteric polymers was the aim of research, which offered the ability of application.[24] T_g value is highly sensitive to the polymer backbone and is profoundly influenced by many secondary forces. Much research in the field of cholesteric liquid-crystalline polymers (LCPs) had been done by our team.[21–23] And the lower T_g cholesteric polymers had been obtained with long carbochain and nonmesogenic chiral group. In this study, long flexible chain is introduced and the polymers with lower glass transition temperature were expected.

For the above-mentioned aims, a new side-chain chiral LCP were synthesized derived from two new

This article contains supplementary material available via the Internet at http://www.interscience.wiley.com/jpages/0021-8995/suppmat

Correspondence to: B.-Y. Zhang (baoyanzhang@hotmail.com).

Contract grant sponsors: China Postdoctoral Science Foundation, Postdoctoral Science and Research Foundation of Northeastern University. Shen Yang Scientific and Technical Bureau Foundation for financial support of this work.

monomers: smectic-nematic liquid crystal monomer: heptyloxy-undecanoyl-oxybiphenyl-4-benzoate ($\mathbf{M_1}$); and chiral nonmesogenic monomer: isosorbide 2-(4-allyloxybenzoyl-5-(4-heptylbenzoyl)biester) ($\mathbf{M_2}$). The aim of this work is to research the effect of the chiral moiety on the phase behavior of copolymers and chiral smectic C phase, and lower T_g values LC polymers were expected simultaneously. The influence of the contents of the chiral agent and the structures of mesogenic on the phase behavior is discussed, and the change trend of optical rotation is also studied.

EXPERIMENTAL

Materials

Polymethylhydrosiloxane (PMHS, M_n = 700–800) was purchased from Jilin Chemical Industry (Jilin, China). 4,4′-Biphenol was purchased from Beijing Chemical Industry (Beijing, China). 3-Bromopropene was purchased from Beijing Fuxing Chemical Industry (Beijing, China). Isosorbide was bought from Yangzhou Shenzhou new material (Yangzhou, China). 1-Bromoheptene was got from Yancheng Longsheng Fine Chemical Industry (Yancheng, China). Ethyl 4-hydroxyl benzoate was purchased from Shenyang Xinxi Chemical Reagent Company (Shenyang, China). Undecylenic acid was purchased from Beijing Jinlong Chemical Reagent (Beijing, China). Toluene used in the hydrosilication reaction was first dried over sodium and then distilled under nitrogen. All other solvents and reagents were purified by standard methods.

Measurement

Specific rotation was performed with Perkin Elmer 341 polarimeter. Phase transition temperatures and thermodynamic parameters were determined by using a Netzsch DSC 204 (Netzsch, Germany) with a liquid nitrogen cooling system. The heating and cooling rates were 10°C/min. A Leica DMRX (Leica, Germany) polarizing optical microscope (POM) equipped with a Linkam THMSE-600 (Linkam, England) hot stage was used to observe phase transition temperatures and analyze LC properties for the monomers and polymers through observation of optical textures. X-ray diffraction (XRD) measurements were performed with a nickel-filtered Cu Kα (λ = 0.1542 nm) radiation with a DMAX-3A Rigaku (Rigaku, Japan) powder diffractometer. IR spectra were measured on a Perkin Elmer spectrum one FTIR spectrometer (Perkin Elmer Instruments, USA). ^{1}H NMR spectra (300 MHZ) were recorded on a Varian WH-90PFT spectrometer. Molecular weight of the polymers were determined by gel permeation chromatography of the polymer solution in toluene using a Waters 2695 separations module equipped with styragel columns and a Waters 2414 refractive-index detector connected in series, at a flow rate of 1 mL/min, and polystyrenes of low polydispersity as standards.

Synthesis of the olefinic compounds

The synthesis of the olefinic compounds is shown in Scheme 1.

Heptyloxy 4-undecanoyloxybiphenyl-4′-benzoate (M_1)

4-Heptyloxybenzoxy-4′-hydroxy biphenyl. 4,4′-Hydroxybiphenyl (93 g, 0.5 mol) was dissolved in mixture of tetrahydrafunan (300 mL) and pyridine (15 mL), and then 25.6 g (0.1 mol) of 4-heptyloxybenzoic acid chloride (laboratory synthesized) was added dropwise to the cold mixture. After refluxing for 15 h, the cold reaction mixture was precipitated into water and acidified to pH = 3–4 with dilute hydrochloric acid. The resulting precipitate was filtered and washed with water to neutrality. After being washed three times in 3% dilute alkali liquor, the crude product was washed with water and recrystallized from acetone. The white solid powders were obtained. Yield: 47.5%, mp: 209°C.

IR (KBr): 3404 (—OH), 2980–2850 (—CH_3, —CH_2), 1728 (C=O), 1605–1450 (Ar—).

Heptyloxy 4-undecanoyloxybiphenyl-4′-benzoate (M_1). A few drops of *N*,*N*-dimethylfomamide (DMF) were

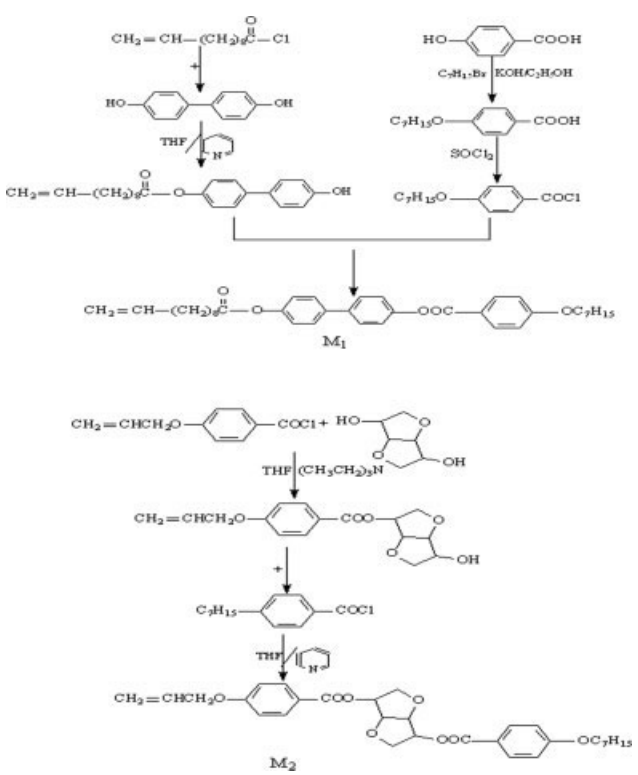

Scheme 1 Synthetic routes of monomer $\mathbf{M_1}$ and $\mathbf{M_2}$.

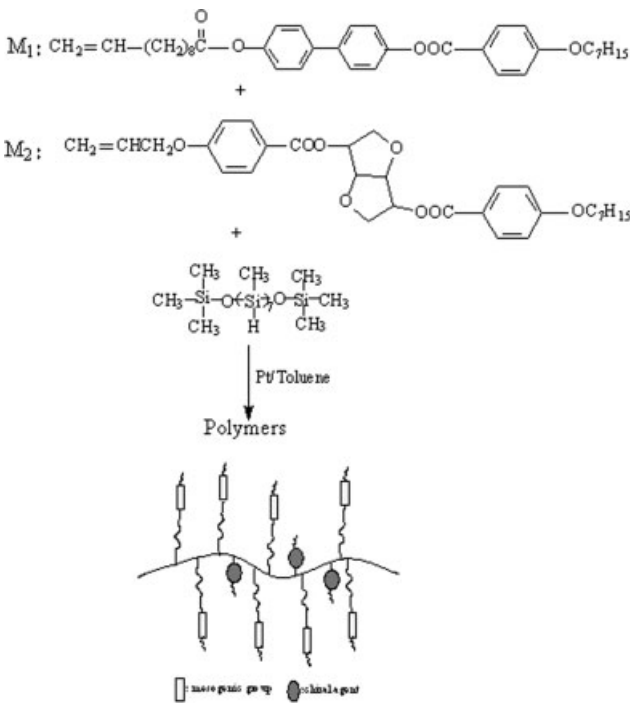

Scheme 2 Synthesis and schematic representation of polymers.

added to a suspension of undecanoic acid (150 mL) with few inhibitor in freshly distilled thionyl chloride (40 mL) and the reaction mixture was refluxed for 5 h and then the excess thionyl chloride was removed under reduced pressure, collecting distillation cut at 129–131°C/1.33 KPa to give the corresponding acid chloride. After 4-hepyloxybenzoxy-4′-hydroxy biphenyl (0.1 mol) had been dissolved in a mixture of anhydrous pyridine (10 mL) and tetrahydrofunan (100 mL), the undecanoic acid chloride was then added at once and the reaction mixture was refluxed for 24 h. The cold reaction mixture was precipitated into water, isolated by filtration and then recrystallized from ethanol. Yield: 65%, mp. 65.7°C.

IR (KBr): 3090 (=C—H), 2980–2850 (—CH_3, —CH_2), 1746, 1727 (C=O), 1648 (C=C), 1605–1450 (Ar—), 1258 cm^{-1} (C—O—C).

^{1}H NMR ($CDCl_3$): δ 0.89–0.92 (t, 3H, —C***H***$_3$), 1.33–1.83 (m, 22H, — (C***H***$_2$)$_6$—, —(C***H***$_2$)$_5$—), 2.04–2.06 (m, 2H, CH_2=CHC***H***$_2$), 2.56–2.60 (t, 2H, —C***H***$_2$COO), 4.03–4.07 (t, 2H, —OC***H***$_2$—), 4.93–5.03 (m, 2H, C***H***$_2$=CH—), 5.78–5.81 (m, 1H, CH_2=C***H***—), 6.88–8.17 (m, 12H, Ar—***H***).

Synthesis of isosorbide 2-(4-allyloxybenzoyl)-5-(4-heptylbenzoyl)biester) (M_2)

Isosorbide 4-allyloxy benzoxy monoester(0.1 mol) (laboratory synthesized) was dissolved in a mixture of anhydrous tetrahydrofunan (200 mL) and pyridine (10 mL), 4-heptyloxy-benzoic acid chloride (0.1 mol) was then added at once and the reaction mixture was refluxed for 30 h. The cold reaction mixture was precipitated into water, acidated, filtered, and washed into neutrality and then obtained from ethanol. The product was obtained in 78% yield, mp: 79°C.

IR (KBr): 3072 (=C—H), 2980–2850 (—CH_3, —CH_2), 1720 (C=O), 1645 (C=C), 1605–1450 cm^{-1} (Ar—).

^{1}H NMR ($CDCl_3$): 0.88–0.91 (t, 3H, —C***H***$_3$), 1.30–1.81 (m, 10H, —C***H***$_2$—), 3.99–4.68 (**H** in isosorbide), 4.03–4.06 (d, 2H, —OC***H***$_2$—), 4.59–5.46 (d, 2H, CH_2=CHC***H***$_2$O), 5.40–5.46 (m, 2H, C***H***$_2$=), 6.05–6.12 (m, 1H, CH_2=C***H***—), 6.88–8.06 (m, 12H, Ar***H***).

Synthesis of the polymers

The synthetic route of polymers is outlined in Scheme 2. The mesogenic monomer and chiral agent reacted with Si—H of PMHS to form polymers in the presence of a Pt catalyst. All the synthesized polymers and the optical activity and average molecule weight are listed in Table I. The monomers **M_1**, **M_2**, and PMHS were dissolved in dried, freshly distilled toluene. The mixture was heated to 65°C under nitrogen and anhydrous conditions, and then 1.5-mL THF solution of hexchloroplatinate(IV) hydrate catalyst (5 mg/mL) was injected with a syringe. The hydrosilylation reaction, followed the track of the Si—H stretch intensity by Fourier transform infrared (FTIR), was completed when the stretch vibrate of Si—H disappeared. The polymers were obtained with methanol, and then were dried in a vacuum at room temperature.

IR (KBr): 2924, 2853 (—CH_3, —CH_2), 1757, 1731 (C=O), 1606–1450 (Ar—), 1200–1000 cm^{-1} (Si—O—Si).

RESULTS AND DISCUSSION

Synthesis

A smectic liquid-crystalline monomer (**M_1**), a chiral agent (**M_2**), and a series of chiral LC polymers

TABLE I
Polymerization, Rotation Activity, and Molecular Weight of P_0–P_7

Polymer	Feed (mmol)		**M_2** (mol %)[a]	Yield (%)	−α (°)[b]	M_w
	M_1	**M_2**				
P_0	3.500	0.000	0	83.6	–	4,790
P_1	3.360	0.140	4	89.2	7.8	4,777
P_2	3.240	0.260	8	85.0	7.9	4,764
P_3	3.000	0.500	14.3	90.1	8.1	4,744
P_4	2.800	0.700	20	87.3	10.0	4,726
P_5	2.500	1.000	28.6	82.6	11.4	4,698
P_6	2.000	1.500	42.9	79.8	13.4	4,652
P_7	1.500	2.000	57.1	83.5	29.5	4,606

[a] Molar fraction of **M_2** based on **M_1** + **M_2**.
[b] Rotation activity of polymers(chloroform as solution).

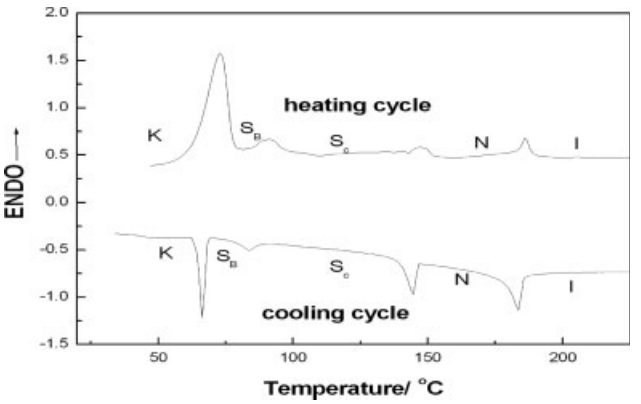

Figure 1 DSC thermographs of liquid crystal monomer $\mathbf{M_1}$.

containing $\mathbf{M_1}$ and $\mathbf{M_2}$ were prepared. The detailed synthetic routes have been shown in Schemes 1 and 2. $\mathbf{M_1}$ was prepared through reacting undecenyl acid chloride with 4-hepyloxybenzoxy-4′-hydroxy biphenyl, and $\mathbf{M_2}$ was obtained by reacting 4-heptyloxy-benzoic acid chloride with isosorbide 4-allyloxy benzoxy monoester. The chemical structures of the two monomers were characterized by FTIR and ^{1}H NMR spectroscopy. The FTIR of $\mathbf{M_1}$ and $\mathbf{M_2}$, respectively, showed characteristic bands at 1746–1720 (cm^{-1}) originating from ester C=O stretching, 1648–1645 (cm^{-1}) due to olefinic C=C stretching and 1605–1450 (cm^{-1}) corresponding to aromatic C=C stretching. The ^{1}H NMR spectra of $\mathbf{M_1}$ and $\mathbf{M_2}$ showed multiplet at 6.88–8.18, 4.93–6.12, 4.58–5.46, 4.00–4.07, 3.99–4.68, 0.88–2.60 ppm corresponding, respectively, to aromatic, vinyl, allyl, methyleneoxy, isosorbide and methyl, methylene protons. IR and ^{1}H NMR spectroscopies confirmed the expected structure for these compounds. The new series of polymers $\mathbf{P_0}$–$\mathbf{P_7}$ were prepared by a one-step hydrosilation reaction between Si—H groups of PMHS and olefinic C=C of smectic-nematic monomer and chiral agent in toluene, using hexachloroplatinate as catalyst at 60°C. The structures of the target polymers are described in Scheme 2. The yields and properties of $\mathbf{P_0}$–$\mathbf{P_7}$ are summarized in Table I. The FTIR spectra of $\mathbf{P_0}$–$\mathbf{P_7}$ showed the complete disappearance of Si—H stretching band at 2166 cm^{-1}. Characteristic absorption bands Si—O—Si appeared at 1200–1000 cm^{-1}. In addition, 1757, 1732, 1605–1450 cm^{-1} attaching to the stretching of ester C=O and aromatic confirmed the monomers introducing into polymer chain successfully. It can be concluded that the chemical structures of obtained monomers and polymers are consistent with our expectation.

Polymers $\mathbf{P_0}$–$\mathbf{P_2}$ dissolved badly in toluene, choloroform, and *N*,*N*-dimethy-formamide first, and then dissolved after putting them overnight, while polymers $\mathbf{P_3}$–$\mathbf{P_7}$ dissolved better in the same solvent. The different solubility of polymers may be due to the existence of the physical crosslinking among the long carbon chain of $\mathbf{M_1}$. It is confirmed by the subsequent analyses on phase behaviors.

Thermal characterization

Analysis of monomer M_1

The differential scanning calorimetric (DSC) curve and phase transition temperature of $\mathbf{M_1}$ during heating and cooling runs are shown in Figure 1 and Table II. When a small molecule liquid crystalline is phase transitioned, they have strictly enthalpy changes which is the direct report of degree acting force between liquid-crystalline molecule and ordered arrangement. The heating cycle thermogram clearly showed four endotherms of the phase transition. A melting transition, smectic B to smectic C, smectic C to nematic, and nematic to isotropic phase transition for $\mathbf{M_1}$ appeared at 72.9, 91.6, 146.7, and 186.3°C. On its cooling cycles, the four opposite endotherms of the phase transition can be seen at 185.6, 150.5, 89.9, 65.1°C for isotropic to nematic, nematic to smectic C, smectic C to smectic B, crystallization of $\mathbf{M_1}$. As it is seen from Figure 1, the values of the enthalpy changes from nematic to smectic phase and between the smectic phases are small and revealed that monomer $\mathbf{M_1}$ is in enantiotropy smectic-nematic phase. The phase transition temperatures determined by DSC were consistent with POM observation results.

Analysis of polymers

LCP can be divided into amorphous LCP, semicrystallization LCP, and crystallization LCP. The range

TABLE II
Phase Transition Temperatures of M_1

Monomer		Phase transition in °C[a] (corresponding enthalpy changes in J/g)
$\mathbf{M_1}$	Heating	K 73.1 (37.9) SB 91.2 (13.5) SC 147.3 (2.7) N 186.3 (2.2) I
	Cooling	I189.7 (2.4) N 150.5 (3.7) SC 90.0 (1.0) SB 66.2 (13.1) K

K, solid; N, nematic; S_B, smectic B; S_C, smectic C; I, isotropic.
[a] Peak temperature was taken as the phase transition temperature.

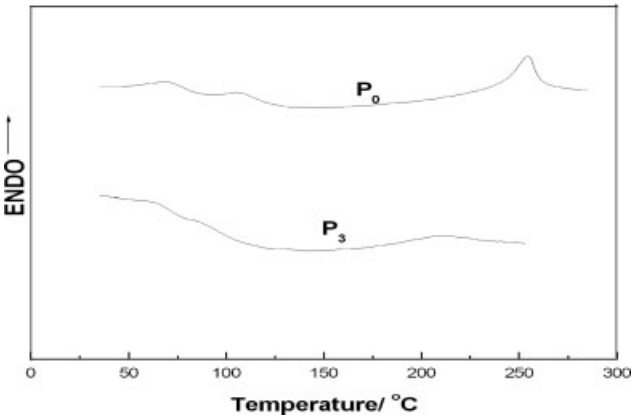

Figure 2 DSC thermographs of liquid crystal polymers.

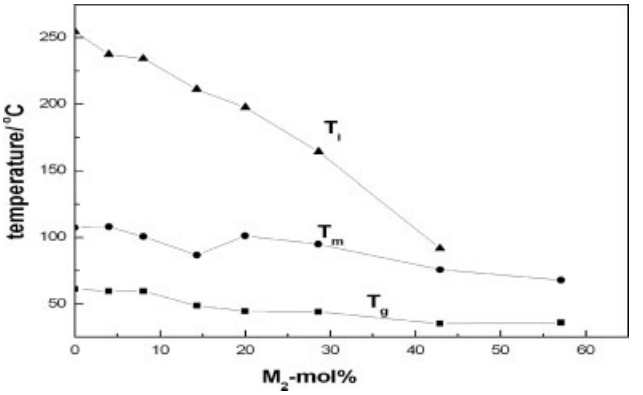

Figure 3 Effect of $\mathbf{M_2}$ content on phase transition temperature of the polymers.

of mesomorphic temperature of semicrystallization and crystallization LCP is between the melting and the clearing temperature. Representative DSC curves of polymer, obtained on the second heating scan, are presented in Figure 2 and phase transition temperature and corresponding enthalpy changes are shown in Table III, and the effect of the content of chiral units on the phase transition are shown in Figure 3.

On the second heating scan of polymers, a glass transition temperature, a melting point, and a temperature of mesophase to isotropic phase transition are shown. All transitions are reversible and do not change on repeated heating and cooling cycles, the phase transition temperatures noted in DSC thermograms are consistent with the mesomorphic transition temperatures observed by POM. It reveals that polymers are semicrystallizable.

At the beginning of molecule design, long carbon chain was introduced into monomer, and polysiloxane were chosen as polymers backbones to synthesize smectic liquid-crystalline monomer and lower glass transition temperature polymers.

The influent factors to T_g are summarized as the property of polymer backbone, the rigidity, sterical hinder, and the interaction force between mesogenic and comonomer uint, the flexible spacer length, and the content of comonomer.

Polysiloxanes backbone and mesogenic and comonomer unit with long, flexible spacer inclines to reduce T_g values, while hard core of mesogenic and comonomer inclines to increase T_g values. In this study, long carbochain exist at the both sides of mesogenic core of $\mathbf{M_1}$, so the interaction of long carbon chain (physical crosslink action) is a significant influence factor which inclines to increase the T_g values. And the dilute action of chiral nonmesogenic monomer $\mathbf{M_2}$ is also the main factor on T_g values which decreases T_g values. When the two factors were considered at the same time, the glass transition temperature given by

$$T_g = T_{g0} + K_1\rho_x - K_2A_d$$

where T_g and T_{g0} are the glass transition temperature of copolymer and homopolymer, K_1, K_2 are constants, ρ_x is the content of the monomer with long carbochain, and A_d is the content of chiral agent.

At the beginning, T_g values of $\mathbf{P_0}$–$\mathbf{P_2}$ changed from 61.1 to 59.5°C. It can be seen that the change is small which is due to equivalent interacting between the physical crosslinking effect and dilute effect. When the dilute effect in the leading role, the T_g values of P_2–P_3 changed abruptly from 59.5 to 48.5°C, and then T_g values of $\mathbf{P_3}$–$\mathbf{P_7}$ decreased smoothly from 48.5 to 35.0°C.

In the DSC curve of $\mathbf{P_0}$–$\mathbf{P_7}$, another peak of heat absorption can be found, which is melting temperature(T_m). Long, flexible carbon chain of mesomorphic monomer and comonomer can easily arrange polymer into order when it possesses crystallization tendency. Along with the change of material ratio the content of $\mathbf{M_1}$ (with long carbon chain) decreased, which brought about the decrease of crystallization ability. While the content of comonomer ($\mathbf{M_2}$) increased, but its structure is not rigid, its crystallization ability also decreased.

TABLE III
Thermal Properties of Polymers P_0–P_7

Polymer	T_g (°C)	T_m (°C)	T_i (°C)	ΔH (J/g)	ΔT[a]	LC phase
P_0	61.1	107.3	254.4	3.96	147.1	S_A
P_1	59.6	108.0	237.3	3.55	129.3	S_A
P_2	59.5	100.6	234.2	2.97	133.6	S_A
P_3	48.5	100.0	211.1	2.50	111.1	Ch
P_4	44.6	101.1	197.4	2.04	96.3	Ch
P_5	44.0	94.9	164.2	0.94	69.3	Ch
P_6	35.1	75.7	91.6	–	–	–
P_7	35.0	67.8	–	–	–	–

[a] Mesophase temperature ranges ($T_i - T_m$).

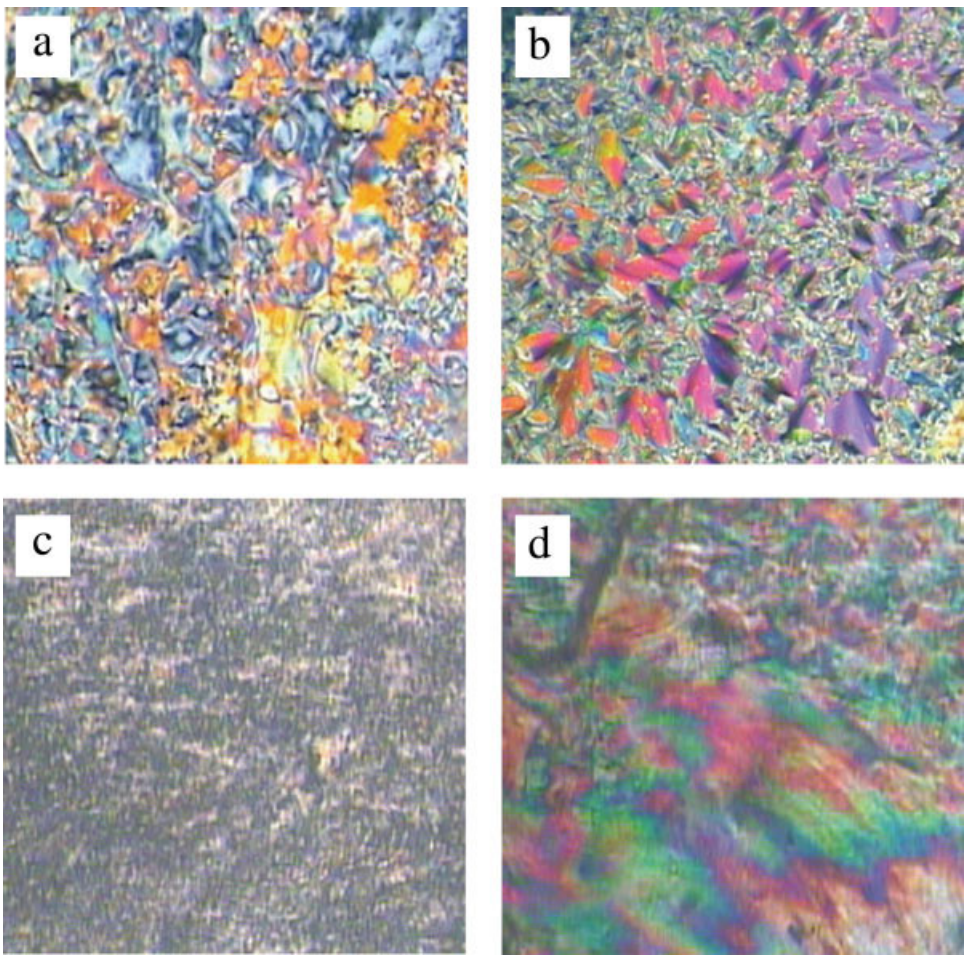

Figure 4 Optical texture of polymers (×200): (a) threaded texture of $\mathbf{M_1}$ at heating to 165.4°C; (b) broken-focal conic texture of $\mathbf{M_1}$ at cooling to 144.5°C; (c) stepped particle texture of $\mathbf{P_2}$ at heating to 154.5°C; and (d) Grandjean texture of $\mathbf{P_4}$ at heating to 183.4°C. [Color figure can be viewed in the online issue, which is available at www.interscience.wiley.com.]

The two factors interacted and T_m values of $\mathbf{P_0}$–$\mathbf{P_7}$ reduced from 107.3 to 67.8°C.

The physical crosslink action of mesogenic monomer and dilute action of chiral agent not only affected T_g of the LCPs but also the isotropization temperature (T_i). The physical crosslink may influence the clearing point (T_i) in two ways. First, may act as a nonmesogenic diluent agent and led to downward shift in the clearing point. Second, heating to the isotropic state required additional energy to distort the polymer backbone from the anisotropic state at physical crosslink and led to forward shift in the clearing point; and the chiral fraction as a dilute agent caused the decrease in T_i values. So the two influent factors interacting control, and the T_i values $\mathbf{P_0}$–$\mathbf{P_6}$ decreased from 254.4 to 164.2°C when the content of the chiral side groups increased from 0 to 28.6 mol %. This indicates that the LC orientation order decreases with increasing the content of the chiral side groups. The mesomorphic properties deteriorated or disappeared when the content of the chiral groups were greater than 30 mol %.

Thermogravimetry can explain well about the stability of the polymers. It will show clearly the point and the degree of the polymer decomposition. It can be obtained by thermogravimetric analyses (TGA). The temperatures at which 5% weight loss occurred (T_d) were greater than 300°C for $\mathbf{P_0}$–$\mathbf{P_7}$, which reveals that the synthesized polymers have a high thermal stability.

LC texture studies

The optical texture of monomer and the polymers were obtained by POM with hot stage under nitrogen atmosphere. The visual observations under POM have revealed that $\mathbf{M_1}$ exhibited enantiotropic smectic-nematic phase. When $\mathbf{M_1}$ was heated to 72.9°C, the sample began to melt and flow and gradually appeared as grainy texture, which is the texture for smectic phase. Continued heating to 146.7°C, the typical nematic threaded texture gradually appeared and remained to 186.3°C. On the cooling cycle, the texture of $\mathbf{M_1}$ underwent threaded texture

at 185.6°C, broken focal-conic texture for S_C phase at 150.5°C, the mosaic texture for S_B phase at 89.9°C and crystallization at 46.5°C. Photomicrographs are shown in Figure 4(a,b) respectively. On the first heating, changes about different smectic phase can not be observed obviously. But on the second heating, the different texture changes of smectic phase were observed just like the first cooling. It should be due to the regular molecular arrangement on the second heating. The results suggested that $\mathbf{M_1}$ showed smectic (S_B, S_C) phase and nematic phase on the heating and the subsequent cooling cycle.

The polymers $\mathbf{P_0}$–$\mathbf{P_2}$ showed typical smectic-stepped particle texture, which may be due to arrangement of long carbochain of $\mathbf{M_1}$ and $\mathbf{M_2}$. Polymers $\mathbf{P_3}$–$\mathbf{P_5}$ exhibited typical cholesteric Grandjean texture. The representative photomicrographs of $\mathbf{P_2}$ and $\mathbf{P_4}$ are shown in Figure 4(c,d). The LC properties of $\mathbf{P_6}$ were not good, while $\mathbf{P_7}$ displayed no liquid-crystalline properties. It can be seen that the LC properties of polymers changed gradually from chiral smectic A to cholesteric phase with the increase content of chiral agent, but when the content of chiral agent is beyond 30%, the LC property of polymers is bad and disappear, which is because of the non-LC chiral agent which first played a chiral role and then a dilute agent when it reached a critical value. The optical rotation values of polymer are listed in Table I, and the change trend of them is shown in Figure 5. From Table I and Figure 5, it can be seen that the optical activities of polymer improved from 7.8 to 29.5 with the increase contents of chiral agent. It can be concluded that chiral agent offered excellent helicity and at the same time provided diluting action.

X-ray diffraction

XRD analysis allowed for a complementary assessment of the nature of the phases observed by DSC and POM, giving additional information about their structural parameters. Wide-angle X-ray diffraction (WAXD) patterns of polymers are shown in Figure 6. In general, a smectic, nematic, and cholesteric structure have a broad peak associated with lateral packing at $2\theta = 16$–21° in WAXD curve. A sharp and strong peak at low angle ($1^\circ < 2\theta < 6^\circ$) in small-angle X-ray scattering curve can be observed for smectic structure, but it cannot be seen for nematic and cholesteric structure. XRD pattern of the quenched polymer $\mathbf{P_0}$–$\mathbf{P_2}$ films showed sharp reflection peaks at 2θ of 4.22, 6.56 (d = 20.91, 13.46 Å), which were corresponding to the smectic layer spacing. The d-value is near to the molecular length of the fully stretched molecule and mesomorphic units which were calculated to 26.48 Å. And the films of $\mathbf{P_3}$–$\mathbf{P_5}$ showed only broad peaks at 2θ of 20.4–22.34 (d = 4.35–3.97 Å). Combining polarizing microscopy with XRD measurements may reveal that polymers $\mathbf{P_0}$–$\mathbf{P_2}$ were chiral smectic A phase, while polymers $\mathbf{P_3}$–$\mathbf{P_5}$ were cholesteric phase.

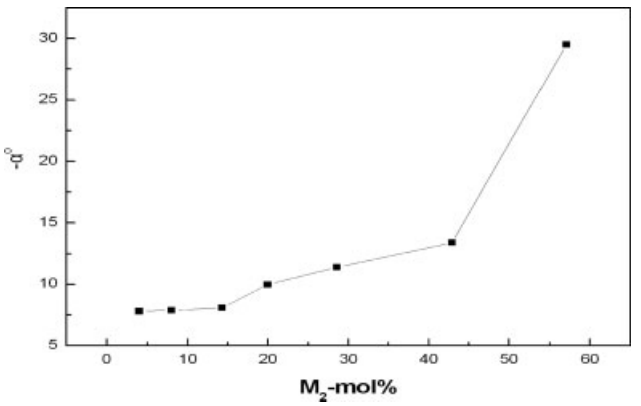

Figure 5 The change trend of rotation activities of polymers.

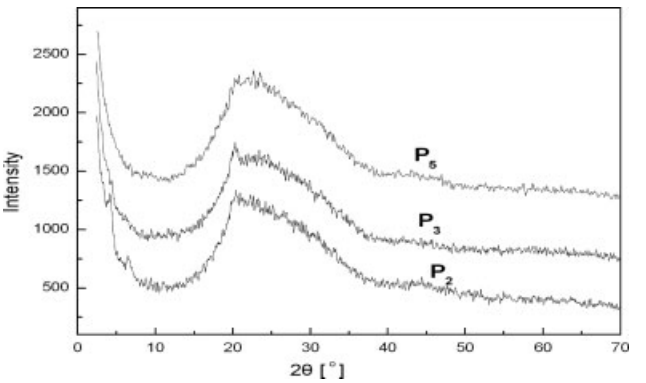

Figure 6 X-ray diffraction patterns of quenched samples.

CONCLUSIONS

In this study, a series of new side-chain chiral LCPs containing smectic-nematic monomer groups heptyloxy-undecanoyl-oxybiphenyl-4-benzoate ($\mathbf{M_1}$) and chiral nonmesogenic monomer isosorbide 2-(4-allyloxybenzoyl-5-(4-heptylbenzoyl) biester) ($\mathbf{M_2}$) were synthesized and characterized. Polymer $\mathbf{P_0}$–$\mathbf{P_2}$ were chiral smectic A phase, while $\mathbf{P_3}$–$\mathbf{P_5}$ were cholesteric phase. The mesomorphic properties deteriorated or disappeared when the content of the chiral groups were greater than 30 mol %. Experimental results demonstrated that nonmesogenic chiral moiety and LC mesogenic with long carbochain offered the possibility of application due to its lower glass transition temperature, and the glass transition temperatures, isotropization temperatures, and the ranges of the mesophase temperature reduced with increasing

the content of chiral agent. All the obtained polymers showed wide mesophase temperature ranges and high thermal stability. And the optical rotation increased with the increase of the chiral agent. Chiral agent offered excellent helicity and provided diluting action simultaneously.

The authors are grateful to National Natural Science Fundamental Committee of China and HI-Tech Research and Development Program (863) of China.

References

1. Zentel, R. Polymer 1992, 33, 4040.
2. Cowie, J. M. G.; Hunter, H. W. J Polym Sci Part A: Polym Chem 1993, 31, 1179.
3. Kim, G. H.; Jin, S.; Pugh, C.; Cheng, S. Z. D. J Polym Sci Part B: Polym Phys 2001, 39, 3029.
4. Bobrovsky, A. Y.; Boiko, N. I.; Shaumburg, K.; Shibaev, V. P. Colloid Polym Sci 2000, 278, 671.
5. Shibaev, P. V.; Chiappetta, D.; Sanford, R. L.; Palffy-Muhoray, P.; Moreira, M.; Cao, W.; Green, M. Macromolecules 2006, 39, 3986.
6. Taton, D.; Borgne, A. L.; Chen, J.; Shum, W. Chirality 1998, 10, 779.
7. Chiellini, E.; Galli, G.; Cioni, F.; Dossi, E. Macromol Chem Macromol Symp 1993, 69, 51.
8. Goodby, J. W. J Mater Chem 1991, 1, 307.
9. Kreuzer, F. H.; Andrejewski, D.; Haas, W.; Harberle, N; Spes, P. Mol Cryst Liq Cryst 1991, 199, 345.
10. Kricheldorf, H. R.; Sun, S. J.; Chen, C. P. J Polym Sci Part A: Polym Chem 1997, 35, 1611.
11. Peter, P. M. Nature 1998, 391, 745.
12. Yang, D. K.; West, J. L.; Chien, L. C.; Doane, J. W. J Appl Phys 1994, 76, 1331.
13. Sapich, B.; Stumpe, J.; Kricheldorf, H. R. Macromolecules 1998, 31, 1016.
14. Broer, D. J.; Finkelman, H.; Kondo, K. Makromol Chem 1988, 189, 185.
15. Jacobs, S. D.; Cerqua, R. A.; Marhsall, K. L.; Schmid, A.; Guardalben, M. J.; Kerrett, K. J Opt Soc Am B 1988, 5, 1962.
16. Mihaha, T.; Nomura, K.; Funaki, K.; Koide, N. Polymer J 1997, 4, 309.
17. Barney, P. L.; Dubois, J. C.; Friedrich, C.; Noel, C.; Polym Bull 1986, 15, 341.
18. Hsiech, C. J.; Wu, S. H.; Hsiue, G. H.; Hsu, C. S. J Polym Sci Part A: Polym Chem 1994, 32, 1077.
19. Stohr, A.; Strohriegl, P. Macromol Chem Phys 1998, 199, 751.
20. Broer, D. J.; Mol, G. N.; Challa, G. Makromol Chem 1989, 190, 19.
21. Zhi, J. G.; Zhang, B. Y.; Zang, B. L.; Shi, G. H. J Appl Polym Sci 2002, 85, 2155.
22. Hu, J. S.; Zhang, B. Y.; Sun, K.; Li, Q. Y. Liq Cryst 2003, 30, 1267.
23. Zhang, B. Y.; Meng, F. B.; He, X. Z.; Lin, D. Liq Cryst 2005, 32, 1161.
24. Deepa, P., Sona, M., Jayakannan, M. J Polym Sci Part A: Polym Chem 2006, 44, 5557.